

Appendix A

Supplemental Tables and Figures for Chapter 2

Supplemental Table 2.1. Primer sequences (SYBR Green assay) used for real-time, quantitative PCR analysis of gene expression (RT-qPCR) and chromatin immunoprecipitation (ChIP) assays.

For RT-qPCR

Xenopus laevis

Dnmt3a mRNA

Forward: 5' GGT CTA TGA AGT GAG GCA GAA GTG 3'

Reverse: 5' TTC AAA CTG CCG CAA GAA ATA C 3'

Alpha-actinin mRNA

Forward: 5' GGA CAA TTA TCC TGC GTT TTG C 3'

Reverse: 5' CCT TCT TTG GCA GAT GTT TCT TC 3'

Mouse

Dnmt3a mRNA

Forward: 5' CCT GTG GTG CAC TGA AAT GG 3'

Reverse: 5' TCG CCA AGC GGC TCA T 3'

GAPDH mRNA

Forward: 5' TGT GTC CGT CGT GGA TCT GA 3'

Reverse: 5' CTT CAC CAC CTT CTT GAT GTC ATC 3'

For ChIP assay

Xenopus laevis

Dnmt3a Region A

Forward: 5' CCC CTC TCT CTG CCC AAC A 3'

Reverse: 5' GTG TCC TTA TTA ACC CCG TTA TCA CT 3'

Dnmt3a Region B

Forward: 5' TGA CTC TGC GCT GCA GTG A 3'

Reverse: 5' AGG CTG CGT CCC CCT TAC 3'

Dnmt3a Region C

Forward: 5' CTC CGT TTC CCC TGC AAA T 3'

Reverse: 5' ACA TAC ACA TTA ATC ACT CCA TTT CCC 3'

Mouse

Dnmt3a +30.1 kb TSS

Forward: 5' CAG AGG AGG GAA CAC TGT ATA A 3'

Reverse: 5' CAA ACA CAA GCC CAG ATG TC 3'

Dnmt3a +39.0 kb TSS (negative control region)

Forward: 5' AGT GAG GCA GGA CTT TCT AGG TAT G 3'

Reverse: 5' ACC TCT GCT TTG CTC CTA CTC AA 3'

Dnmt3a +49.0 kb TSS

Forward: 5' CCA ACT TCC TCC AGG GTT ATT T 3'

Reverse: 5' GCC CTT GCT GGG TTA TTC T 3'

Supplemental Table 2.2. Genomic coordinates of TR binding sites associated with the *dnmt3a* loci identified by high-throughput sequencing analyses

TR ChIA-PET conducted on premetamorphic *Xenopus tropicalis* tail fin (Sachs and colleagues, unpublished data) (coordinates are based on XenTro2 build)

Region A: Scaffold_971: 107,805-108,924

Region B: Scaffold_971: 120,574-120,823

Region C: Scaffold_971: 124,856-125,536

TR ChIP-seq conducted on mouse liver chromatin (Ramadoss et al., 2014) (Mm9 build)

Peak 1: chr12: 3,806,012-3,806,644

Peak 2: chr12: 3,807,928-3,809,079

Peak 3: chr12: 3,812,247-3,813,164

Peak 4 (+30.1 kb TSS): chr12: 3,837,246-?

Peak 5: chr12: 3,841,058-3,841,690

Peak 6: chr12: 3,859,292-3,860,559

Peak 7: chr12: 3,866,399-3,867,232

Peak 8: chr12: 3,868,339-3,869,565

Peak 9: chr12: 3,889,702-3,890,300

Peak 10: chr12: 3,894,480-3,895,087

Peak 11: chr12: 3,911,787-3,912,497

Peak 12: chr12: 3,919,268-3,919,956

TR ChIP-seq conducted on mouse cerebellar cell line C17.2 (Chatonett et al., 2013) (Mm9 build)

Peak 13 (+49.0 kb TSS): chr12: 3,855,855-3,856,520

Supplemental Table 2.3. Oligonucleotides used for plasmid constructs used in transfection-reporter assay and in *in situ* hybridization histochemistry (ISHH); Oligonucleotides used for electrophoretic mobility shift assay (EMSA)

PCR primers used to amplify *X. laevis dnmt3a* cDNA for subcloning into pGEM-Teasy cloning vector

Forward: 5' TTT CCC ATC ATG CCC AGA GAA CGA 3'

Reverse: 5' GCC GTC GTC ATC GTA TTG GT 3'

PCR primers used to amplify genomic fragments for subcloning into pGL4.23/pCpGL luciferase vectors (restriction sites are underlined)

Xenopus tropicalis

Dnmt3a region A (pGL4.23)

Forward: 5' TAT GGT ACC GGG CCC TAC AGA GCA TAT AGT 3'

Reverse: 5' CAA TGA GCT CCA TTT CTG TGA GAC TGC CTA TCC 3'

Dnmt3a region B (pGL4.23)

Forward: 5' AAG GTA CCA CAG TCA GTT CTG CTC ATG TTG GG 3'

Reverse: 5' TTC TCG AGC TGC ACA TAC CCT TCC CTG TGT AT 3'

Mouse

Dnmt3a +30.1 kb TSS (pCpGL)

Forward: 5' CCC AGA TCT TGG GAC AAA CTC CTC TCA TC 3'

Reverse: 5' GCC CAA GCT TGC TCT AGC CTT TGT CTA ACC 3'

Dnmt3a +49.0 kb TSS (pGL4.23)

Forward: 5' AGC GGT ACC GGG ATT TAT ACC CAC CAA CT 3'

Reverse: 5' TGA CGA GCT CCA GCT GTC TTC TGG AAG GCC A 3'

PCR primers used for site-directed mutagenesis of pGL4.23/pCpGL luciferase vectors (lowercase letters indicate mutated nucleotides)

Xenopus tropicalis

Dnmt3a T₃RE-A1

Forward: 5' CAG AGC GGG GGc TAG CTG AGa ACT GGC CTG CA 3'

Reverse: 5' TGC AGG CCA GTt CTC AGC TA_g CCC CCG CTC TG 3'

Dnmt3a T₃RE-B2

Forward: 5' CCC CAG TGG GTT AtC TGG TTT GgC TCT GCG CTG CA 3'

Reverse: 5' TGC AGC GCA GAG cCA AAC CAG aTA ACC CAC TGG GG 3'

Mouse

Dnmt3a +30.1 kb T₃RE 2

Forward: 5' CTG CCT CTT CAG GtA GAT GTG ACT aCA GGA CAT CTG GG 3'
Reverse: 5' CCC AGA TGT CCT GtA GTC ACA TCT aCC TGA AGA GGC AG 3'

Dnmt3a +30.1 kb T₃RE 3

Forward: 5' GCC TCT TCA GGG AGA TaT GAC TTC AGa ACA TCT GGG CTT G 3'
Reverse: 5' CAA GCC CAG ATG TtC TGA AGT CA_t ATC TCC CTG AAG AGG C 3'

Dnmt3a +30.1 kb T₃RE 4

Forward: 5' GGA GAT GTG ACT TCA GaA CAT CTG GaC TTG TGT TTG CTC AGC 3'
Reverse: 5' GCT GAG CAA ACA CAA GtC CAG ATG TtC TGA AGT CAC ATC TCC 3'

Dnmt3a +30.1 kb T₃RE 6

Forward: 5' GCC TGT GGA AGc CAG CTG AGa TCA CGG GCA GG 3'
Reverse: 5' CCT GCC CGT GA_t CTC AGC TGg CTT CCA CAG GC 3'

Dnmt3a +49.0 kb T₃RE wild-type

Forward: 5' GGG TGC ATT CTG AGG cCA CTC TTG aTA AGA ATA ACC CAG C 3'
Reverse: 5' GCT GGG TTA TTC TTA tCA AGA GTG gCC TCA GAA TGC ACC C 3'

Oligonucleotides used for EMSA (lowercase letters indicate non-native nucleotides added to the 5' ends for [³²P] labeling by Kelnow fill-in)

Xenopus tropicalis

Dnmt3a T₃RE-A1 wild-type

Forward: 5' gat cAC AGA GCG GGG GTT AGC TGA GGA CTG GCC TGC AC 3'
Reverse: 5' gat cGT GCA GGC CAG TCC TCA GCT AAC CCC CGC TCT GT 3'

Dnmt3a T₃RE-A1 mutant (mutated sequence is underlined)

Forward: 5' gat cAC AGA GCG GGG GCT AGC TGA GAA CTG GCC TGC AC 3'
Reverse: 5' gat cGT GCA GGC CAG TTC TCA GCT AGC CCC CGC TCT GT 3'

Dnmt3a T₃RE-B2 wild-type

Forward: 5' gat cTG CAG CGC AGA GTC AAA CCA GGT AAC CCA CTG GG 3'
Reverse: 5' gat cCC CAG TGG GTT ACC TGG TTT GAC TCT GCG CTG CA 3'

Dnmt3a T₃RE-B2 mutant (mutated sequence is underlined)

Forward: 5' gat cTG CAG CGC AGA GCC AAA CCA GAT AAC CCA CTG GG 3'
Reverse: 5' gat cCC CAG TGG GTT AIC TGG TTT GGC TCT GCG CTG CA 3'

Mouse

Dnmt3a +30.1 kb T₃RE 1

Forward: 5' gat cCG CTT TGA AGC AGA GGA GGG AAC ACT GTA T 3'
Reverse: 5' gat cAT ACA GTG TTC CCT CCT CTG CTT CAA AGC G 3'

Dnmt3a +30.1 kb T₃RE 2-4

Forward: 5' gat cCT TCA GGG AGA TGT GAC TTC AGG ACA TCT GGG CTT GTG TTT 3'

Reverse: 5' gat cAA ACA CAA GCC CAG ATG TCC TGA AGT CAC ATC TCC CTG AAG 3'

Dnmt3a +30.1 kb T₃RE 5

Forward: 5' gat cGT AAC TCT AGC CTT GCC TGT CTT ACA GGG C 3'

Reverse: 5' gat cGC CCT GTA AGA CAG GCA AGG CTA GAG TTA C 3'

Dnmt3a +30.1 kb T₃RE 6

Forward: 5' gat cCC TGT GGA AGT CAG CTG AGG TCA CGG GCA G 3'

Reverse: 5' gat cCT GCC CGT GAC CTC AGC TGA CTT CCA CAG G 3'

Dnmt3a +30.1 kb T₃RE 7

Forward: 5' gat cAG ATT CTG GGA CTG ATA GAG TGA GCG TAT T 3'

Reverse: 5' gat cAA TAC GCT CAC TCT ATC AGT CCC AGA ATC T 3'

Dnmt3a +49.0 kb T₃RE wild-type

Forward: 5' gat cGT GCA TTC TGA GGT CAC TCT TGC TAA GAA TAA CCC A 3'

Reverse: 5' gat cTG GGT TAT TCT TAG CAA GAG TGA CCT CAG AAT GCA C 3'

Dnmt3a +49.0 kb T₃RE mutant (mutated sequence is underlined)

Forward: 5' gat cGT GCA TTC TGA GGC CAC TCT TGA TAA GAA TAA CCC A 3'

Reverse: 5' gat cTG GGT TAT TCT TAT CAA GAG TGG CCT CAG AAT GCA C 3'

PCR primers used to generate genomic fragments for competitive EMSA

Xenopus tropicalis

Region A with T₃RE-A1 (wild-type and mutant)

Forward: 5' GCC CTA CAG AGT AAT GTT GCT TAT 3'

Reverse: 5' CCT CAC TCT GCC GTC ATC TA 3'

Region A with T₃RE-A2

Forward: 5' ACT TCC CAG TTT GCC CTC T 3'

Reverse: 5' AAA GCT GCT TCC CAC AAT CC 3'

Region A with T₃RE-A3

Forward: 5' TAT CGG GCA CAC TGG TAC A 3'

Reverse: 5' CCC ACA ACC ACA CTT TCC 3'

Region B with T₃RE-B1

Forward: 5' AAG GTA CCA CAG TCA GTT CTG CTC ATG TTG GG 3'

Reverse: 5' CCC TCC CAT CGC TGC ACT T 3'

Region B with T₃RE-B2 (wild-type and mutant)

Forward: 5' AAG TGC AGC GAT GGG AGG G 3'

Reverse: 5' AAT CAT TCT TGG CTG CGC CC 3'

Region B with T₃RE-B3

Forward: 5' GGG CGC AGC CAA GAA TGA TT 3'

Reverse: 5' CCT GCA CAT ACC CTT CCC TGT GTA T 3'

Region B with no T₃RE

Forward: 5' ATA CAC AGG GAA GGG TAT GTG CAG G 3'

Reverse: 5' TTA CCA AAC TGC AAC TCC CAG CAG 3'

Mouse

+30.1 kb TSS region with T₃RE (wild-type, and mutant 2, 3, 4 and 6)

Forward: 5' CAG AGG AGG GAA CAC TGT ATA A 3'

Reverse: 5' CCC TCA TAA TTG GAC CAG AC 3'

+49.0 kb TSS region with T₃RE (wild-type and mutant)

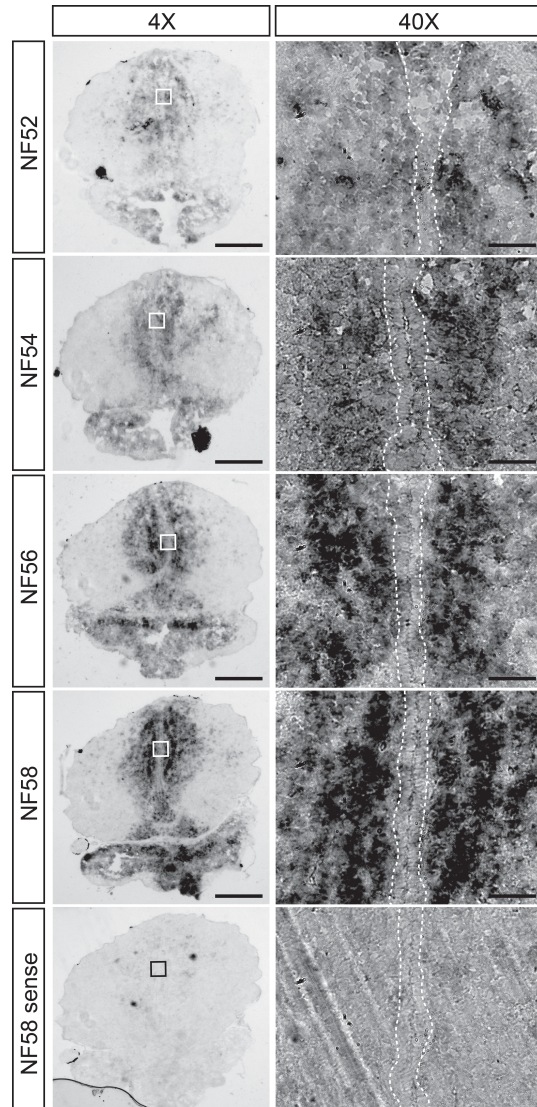
Forward: 5' AGC GGT ACC GGG ATT TAT ACC CAC CAA CT 3'

Reverse: 5' GGC TGC TGT GGA GTA AGT A 3'

+49.0 kb TSS with no T₃RE

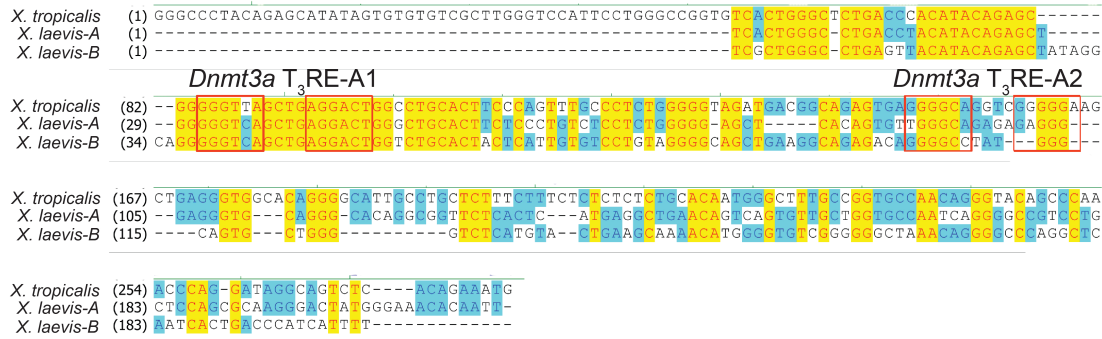
Forward: 5' TAC TTA CTC CAC AGC AGC C 3'

Reverse: 5' CCA AAT GGC TCT TAG ACT GG 3'

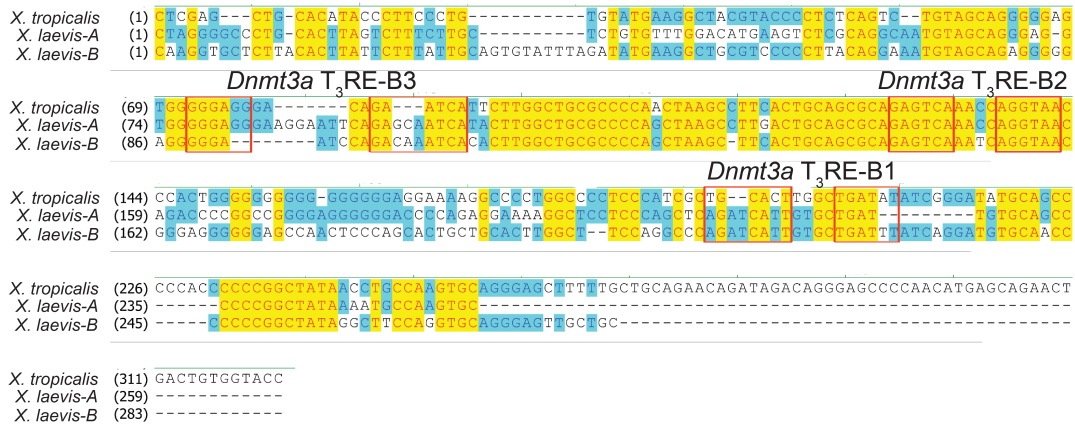


Supplemental Fig. 2.1: *Dnmt3a* mRNA exhibits developmental increases in *Xenopus* tadpole brain. I conducted ISHH for *dnmt3a* mRNA on *X. laevis* tadpole brain between premetamorphosis and late prometamorphosis (NF stages 52 and 58) during metamorphosis. Shown are representative micrographs of transverse sections at the region of the ventral hypothalamus and thalamic nuclei (region 1 in Fig. 1B). Right panels (40X) show magnified view of regions indicated by boxes in left panels. Areas within dotted lines indicate the ventricular and subventricular zones (VZ/SVZ). Note that *dnmt3a* mRNA is excluded from the VZ and SVZ. Scale bar = 200 μ m (4X), 20 μ m (40X).

A.

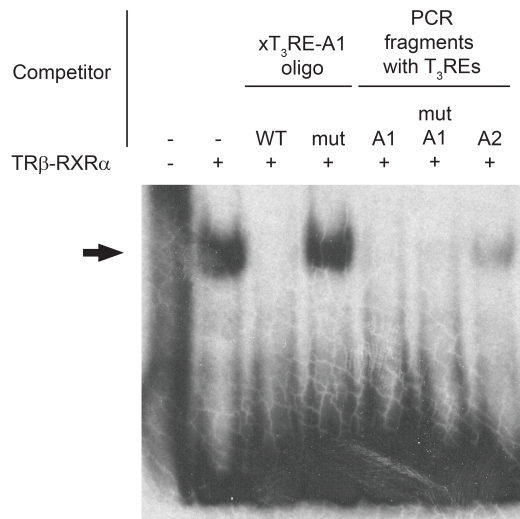


B.

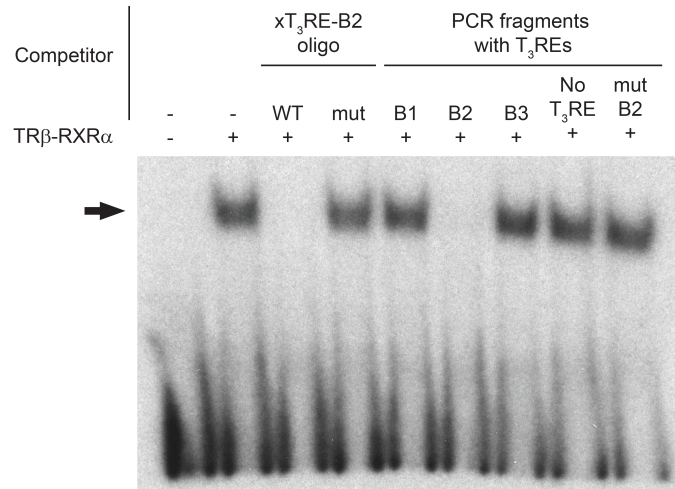


Supplemental Fig. 2.2. Identification of conserved T₃REs associated with the frog *dnmt3a* gene. By analyzing data from a ChIA-PET experiment conducted on tadpole tail fin chromatin with TR as the target protein (L. Sachs and N. Buisine, unpublished data) I identified three putative TR binding sites at the *X. tropicalis dnmt3a* locus (regions A, B and C). Shown are sequence alignment of homologous, conserved genomic loci found in the *X. laevis* genome (Build 5.0) for regions A and B. Alignment for region C is not shown because I did not find TR association at this locus in tadpole brain (see Results and Fig. 2C) and did not further investigate this locus. The *Xenopus laevis* genome is pseudotetraploid (*X. tropicalis* is diploid), and therefore, there are two homologous regions for each region. Boxes indicate the locations of predicted T₃RE half sites based on *X. tropicalis* sequences). The T₃REs are numbered in 5' to 3' direction according to the *X. tropicalis* reference genome (XenTro2 Build). In region A I found another putative T₃RE (xT₃RE-A3), but it is not shown in the alignment because it is located outside the conserved region.

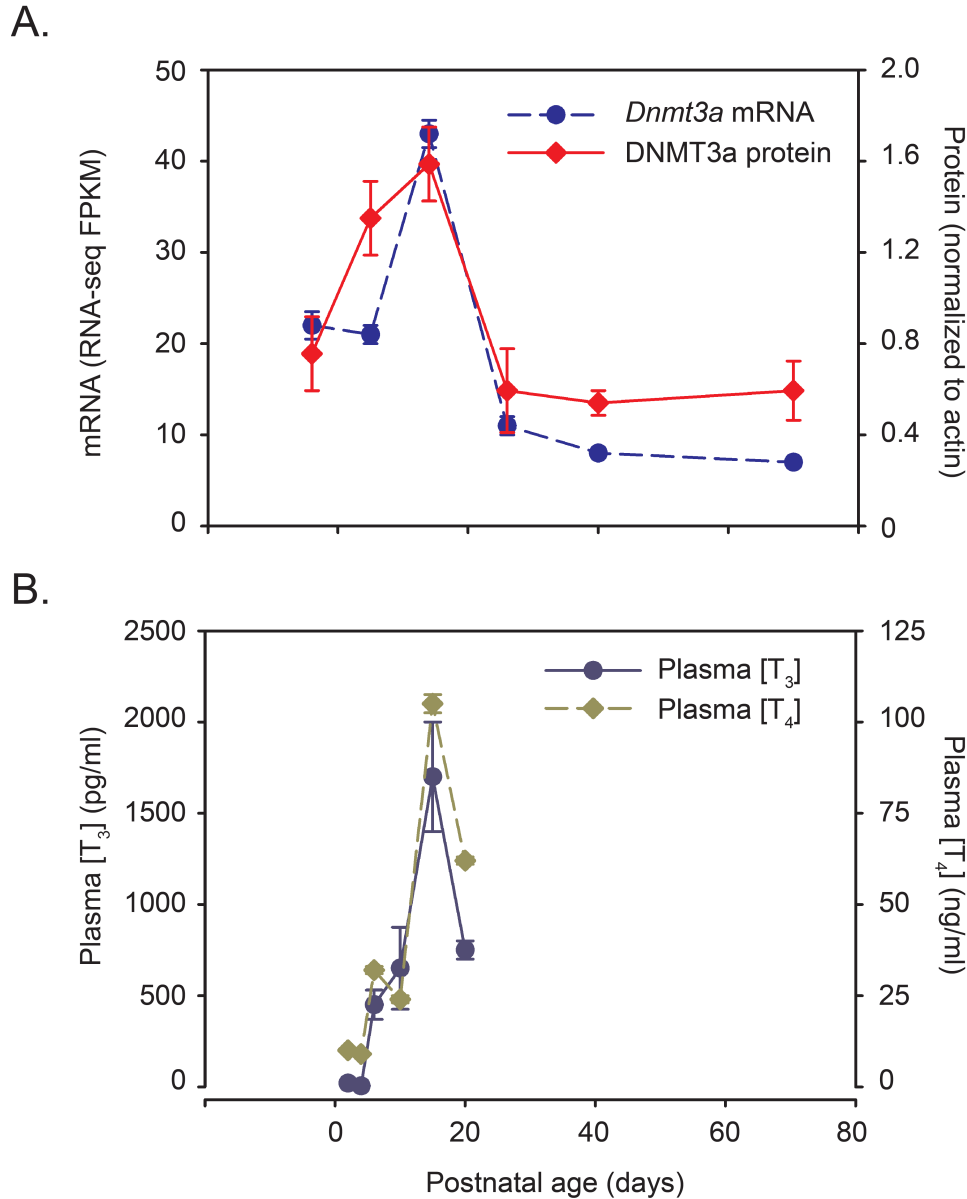
A.



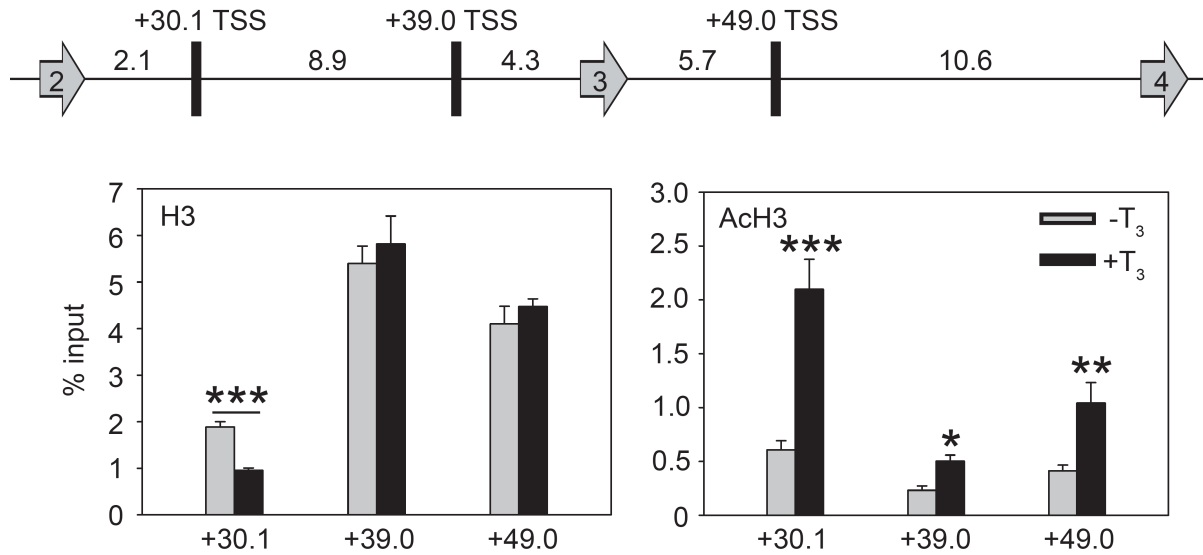
B.



Supplemental Fig. 2.3: Radioinert duplex oligonucleotides or DNA fragments containing the frog *dnmt3a* T₃REs displace TRβ-RXRα from the radiolabeled probe. I conducted competitive EMSA using a [³²P]-labeled oligonucleotide probe corresponding to the xT₃RE-B2 sequences. Before gel electrophoresis the probe was incubated with *in vitro* synthesized *Xenopus* TRβ plus RXRα with or without indicated radioinert oligonucleotides or PCR-generated genomic fragments that encompass the predicted T₃REs (see Supplemental Fig. 2 for location of the predicted T₃REs; probe sequences and primer sequences that were used to generate PCR fragments are given in Supplemental Table 2.2). Mutant oligonucleotides or genomic fragments contained single base pair mutations that were introduced into each of the two half sites of the indicated T₃REs; these mutations abolished T₃-dependent transactivity of regions A and B of the *X. tropicalis dnmt3a* locus (see Results and Fig. 3B). The arrows indicate the location of supershifted bands due to TRβ-RXRα binding to the probes. **(A.)** A radioinert oligonucleotide (1 μM) corresponding to the native xT₃RE -A1 sequence completely displaced TRβ-RXRα binding to the probe, while that for the mutant xT₃RE-A1 did not. Radioinert PCR-generated genomic fragments (19 nM) that encompass the native and mutant xT₃RE-A1 sequences both completely displaced TRβ-RXRα binding to the probe, while that for xT₃RE-A2 sequence had a reduced activity **(B.)** A radioinert oligonucleotide (1 μM) corresponding to the native xT₃RE-B2 sequence completely displaced TRβ-RXRα binding to the probe, while that for the mutant xT₃RE-B2 sequence did not. Radioinert PCR-generated genomic fragments (22 nM) that encompass the native xT₃RE -B2 sequence completely displaced TRβ-RXRα binding to the probe, while those for xT₃RE -B1, xT₃RE -B3 and the mutant xT₃RE -B2 sequences had no activity. A PCR fragment that did not contain a predicted T₃RE was used as a negative control.



Supplemental Fig. 2.4: Developmental increases in *Dnmt3a* mRNA and protein correlate with increase in circulating plasma [T₃] and [T₄] in neonatal mouse. (A.) *Dnmt3a* mRNA and protein levels peak at PND14 in neonatal mouse frontal cortex. The mRNA level was measured using RNA-seq (FPKM, fragments per kilobase of exon per million fragments mapped) and protein level was measured by Western blot (normalized to actin protein) (B.) Circulating plasma [T₃] and [T₄] levels also reach their highest levels at PND14 in mouse as measured by radioimmunoassay. Points represent the mean \pm SEM ($n \geq 4$) (Both figures were adapted and modified with permission from A: Lister et al., (2013); and B: Hadj-Sahraoui et al. (2000)).



Supplemental Fig. 2.5: T₃ treatment reduces histone H3 (H3) and increases acetylated H3 (AcH3) at the +30.1 kb from the TSS of the mouse *Dnmt3a* gene in Neuro2a[TRβ1] cells.

The schematic diagram (top) shows putative TR binding sites (rectangles) identified by TR ChIP-seq experiments conducted on mouse liver (REF) and C17.2 mouse cerebellar cell line (REF) that are located between exons 2 and 4 (arrows) of the mouse *Dnmt3a* gene (distance between features are in kb). I conducted targeted ChIP assays for histone 3 (H3) and acetylated H3 (AcH3) at +30.1, +39.0 and +49.0 kb from the TSS of the mouse *Dnmt3a* gene using chromatin isolated from Neuro2a[TRβ1] cells treated with vehicle (0.1% DMSO) or T₃ (30 nM) for 24 hrs before harvest. Purified IgG antibodies (negative control) yielded < 0.03% of input DNA (data not shown). Bars represent the mean ± SEM ChIP signal expressed as a percentage of input DNA quantity. Asterisks above the means indicate statistically significant differences in ChIP signals between treatments (**p* < 0.05, ***p* < 0.01, ****p* < 0.001; Student's independent sample *t*-test).

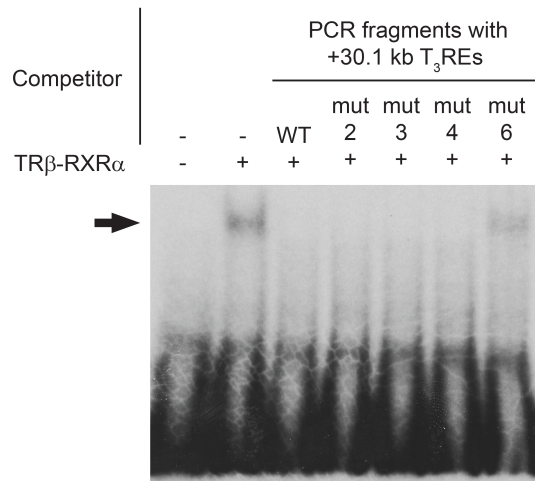
```

CCCCACAGCT GGGACAAACT CCTCTCATCA GACTGTGACC CCATGCTGCA CAGCAGCAAG TCATGTGGTC TCTGTATTGT
GGATAGTTCG CTTTGAAGCA GAGGAGGGAA CACTGTATAA GAAATCAGAA GTCCCAGGCC CCAACGCTGG GGCTGCCTCT
1
TCAGGGAGAT GTGACTTCAG GACATCTGGG CTTGTGTTTG CTCAGCTGGA AAATGGGGAT AGTAACTCTA GCCTTGCCTG
2 3 4 5
TCTTACAGGG CGCCTGTGGA AGTCAGCTGA GGTCACGGGC AGGGAAGTGC CCTGCAGACA GCAAAGTCTG GTCCAATTAT
6
GAGGGATTAC GATTGCTATT ATTATCTACC CATAGTAACT GCTCTGGCTC TGGTGGCAAC AAACACACGC CCAGACCTAG
ATTCTGGGAC TGATAGAGTG AGCGTATTTCG CATACTGGCA GGGGCCATTA TACCAAAGA TGACAGCAAT CTGGTTAGAC
7
AAAGGCTAGA GCCTGGCTGG G

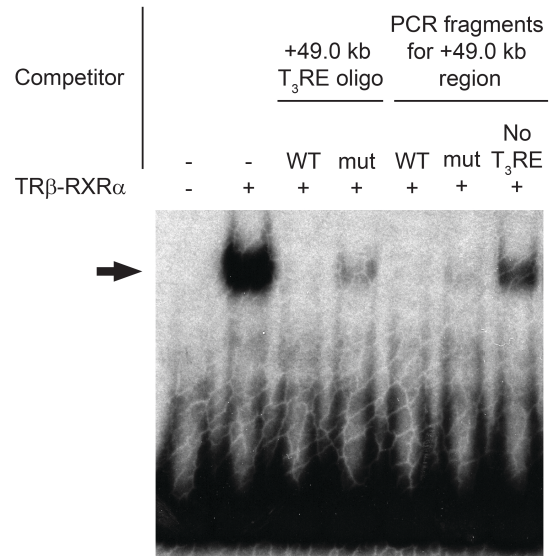
```

Supplemental Fig. 2.6: Identification of putative T₃REs in +30.1 kb TSS region of the mouse *Dnmt3a* gene. Shown is the DNA sequence of the 500 bp region centered at +30.1 kb from the TSS of the mouse *Dnmt3a* gene and location of the seven predicted T₃REs (underlined) found within this region. Oligonucleotide sequences for competitive EMSA in Fig. 6A were designed to encompass these predicted T₃REs (Supplemental Table 2.2).

A.

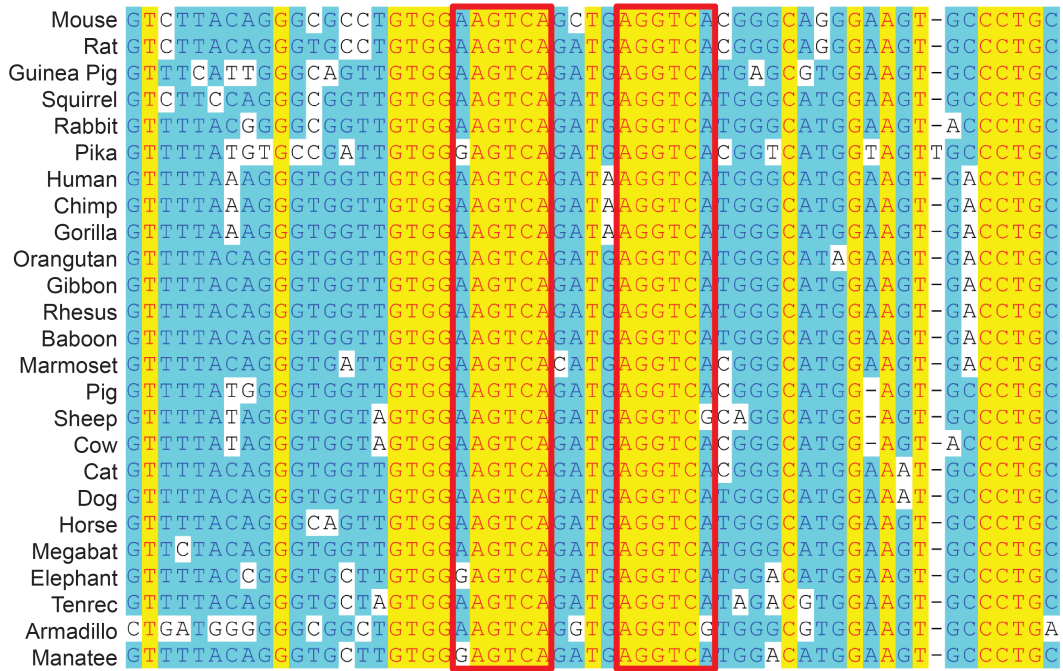


B.

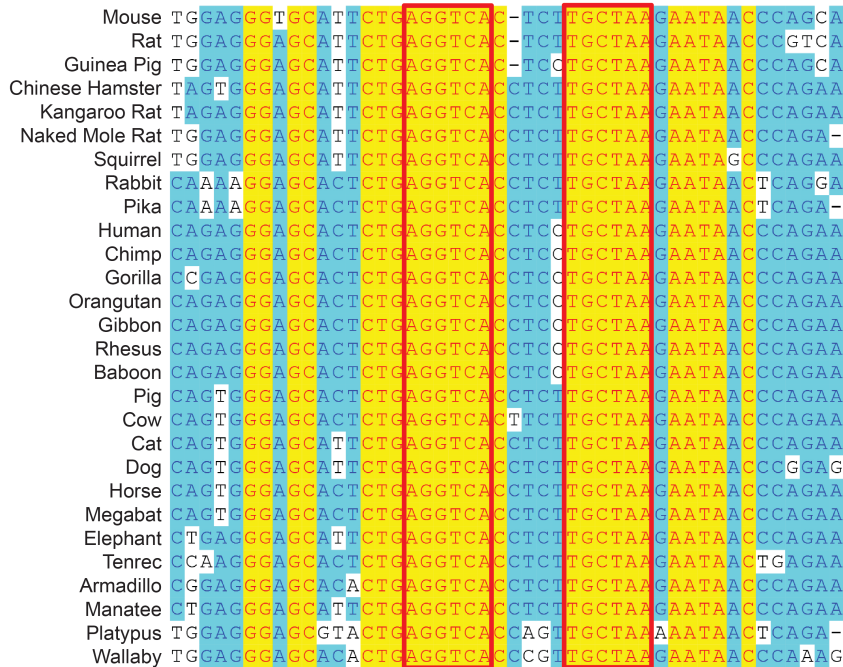


Supplemental Fig. 2.7: Radioinert oligonucleotides or DNA fragments that encompass the predicted mouse *Dnmt3a* T₃REs displaces TRβ-RXRα heterodimers from the radiolabeled probe (A.) I conducted competitive EMSA using a [³²P]-labeled oligonucleotide probe corresponding to the *X. tropicalis dnmt3a* xT₃RE -B2 sequence (probe) and radioinert PCR-generated genomic fragments (277 bp) that encompass the sequences of putative T₃RE s 2, 3, 4 and 6 found within a 500 bp genomic region centered at +30.1 kb from the TSS of the mouse *Dnmt3a* gene (see Supplemental Fig. 6 for location of these predicted T₃REs; primer sequences that were used to generate PCR fragments are given in Supplemental Table 2.2). Mutant PCR fragments contained single base pair mutations that were introduced into each of the two half sites of the indicated T₃REs. Mutations of T₃REs 2, 3 and 4 reduced T₃-dependent transactivity of the +30.1 kb region, while mutation of T₃RE 6 almost completely abolished it (see Results and Fig. 6B). Before gel electrophoresis the probe was incubated with *in vitro* synthesized *Xenopus* TRβ plus RXRα with or without the indicated radioinert PCR fragments (21.5 nM). The arrow indicates the location of supershifted bands due to TRβ-RXRα binding to the probe. Radioinert PCR fragments that contained native T₃RE sequences and those for the mutant T₃RE 2, 3, and 4 completely displaced TRβ-RXRα binding to the probe, while that for mutant T₃RE 6 had a reduced activity. **(B.)** I conducted competitive EMSA using the probe and radioinert oligonucleotides corresponding to the mouse +49.0 kb T₃RE sequence (1 μM) or PCR-generated genomic fragments (180 bp) that encompass correspond the mouse +49.0 kb T₃RE. The arrow indicates the location of supershifted bands due to TRβ-RXRα binding to the probe. Mutant PCR fragments contained single base pair mutations that were introduced into each of the two half sites of the +49.0 kb T₃RE, which reduced T₃-dependent transactivity of the +49.0 kb region (see Results and Fig. 6D). Radioinert oligonucleotide with the native sequence completely displaced TRβ-RXRα binding to the probe, while that for mutant sequence had a reduced activity. Radioinert PCR fragment (34 nM) that contained the native +49.0 kb T₃RE sequence completely displaced TRβ-RXRα binding to the probe, while that for the mutant sequence reduced TRβ-RXRα binding to the probe. A PCR fragment that did not contain a predicted T₃RE was used as a negative control, which did not have activity.

A.



B.



Supplemental Fig. 2.8: Sequence conservation of mouse *Dnmt3a* T₃REs among mammals. Shown are DNA sequence alignment of T₃REs found at the +30.1 kb (A.) and +49.0 kb (B.) from the TSS of the mouse *Dnmt3a* gene. Boxes indicate the location of predicated T₃RE half sites based on the mouse sequences. Note that the +49.0 kb T₃RE is DR+4 for mouse, rat and Chinese hamster, while it is DR+5 for other species.